

AFML-TR-72-103

AD 749932

**IMPORTANCE OF SLIP MODE FOR  
DISPERSION-HARDENED BETA TITANIUM ALLOYS**

**T. HAMAJIMA, G. LÜTJERING and S. WEISSMANN**

**RUTGERS UNIVERSITY**

*The State University of New Jersey*

**TECHNICAL REPORT AFML-TR-72-103**

D D C  
RECORDED  
OCT 10 1972  
RECORDED  
C

**JULY 1972**

Reprinted by  
NATIONAL TECHNICAL  
INFORMATION SERVICE  
U.S. GOVERNMENT PRINTING OFFICE  
WASHINGTON, D.C. 20540

Approved for public release; distribution unlimited.

Details of illustrations in  
this document may be better  
studied on microfiche

**AIR FORCE MATERIALS LABORATORY  
AIR FORCE SYSTEMS COMMAND  
WRIGHT-PATTERSON AIR FORCE BASE, OHIO**

NOTICE

When Government drawings, specifications, or other data are used for any purpose other than in connection with a definitely related Government procurement operation, the United States Government thereby incurs no responsibility nor any obligation whatsoever; and the fact that the government may have formulated, furnished, or in any way supplied the said drawings, specifications, or other data, is not to be regarded by implication or otherwise as in any manner licensing the holder or any other person or corporation, or conveying any rights or permission to manufacture, use, or sell any patented invention that may in any way be related thereto.

ACCESSION for	
NTIS	White Section <input checked="" type="checkbox"/>
GPO	Buff Section <input type="checkbox"/>
UNANNOUNCED	<input type="checkbox"/>
JUSTIFICATION .....	
BY .....	
DISTRIBUTION/AVAILABILITY CODES	
Dist.	AvAIL. Sec. or SPECIAL
A	

Copies of this report should not be returned unless return is required by security considerations, contractual obligations, or notice on a specific document.

UNCLASSIFIED

Security Classification

DOCUMENT CONTROL DATA - R & D

Security Classification of title, body of abstract and indexing annotation must be entered when the overall report is classified

ORIGINATING ACTIVITY (Corporate Author)  
Rutgers University, The State University of New Jersey  
Materials Research Laboratory  
Bureau of Engineering Research  
New Brunswick, New Jersey 08903

2a. REPORT SECURITY CLASSIFICATION

Unclassified

2b. GROUP

3. REPORT TITLE

IMPORTANCE OF SLIP MODE FOR DISPERSION-HARDENED BETA TITANIUM ALLOYS

4. DESCRIPTIVE NOTES (Type of report and inclusive dates)

Final Report, October 1, 1971--March 31, 1972

5. AUTHOR(S) (First name, middle initial, last name)

T. Hamajima, G. Lütjering and S. Weissmann

6. REPORT DATE

July, 1972

7a. TOTAL NO. OF PAGES

13

7b. NO. OF REFS

9

8a. CONTRACT OR GRANT NO

AF33615-69-C-1322

b. PROJECT NO.

7353

c. Task No. 735302

d.

9a. ORIGINATOR'S REPORT NUMBER(S)

9b. OTHER REPORT NO(S) (Any other numbers that may be assigned this report)

AFML-TR-72-103

10. DISTRIBUTION STATEMENT

Approved for public release; distribution unlimited.

11. SUPPLEMENTARY NOTES

12. SPONSORING MILITARY ACTIVITY

Air Force Materials Laboratory  
Air Force Systems Command  
Wright-Patterson Air Force Base, Ohio

13. ABSTRACT

The mechanical properties of Ti-7 Mo-7 Al and Ti-7 Mo-16 Al (in atomic per cent) were correlated to the microstructure. The mechanical properties of the alloy with low aluminum content, consisting of  $\alpha + \beta$  phases, were dependent on the size of the  $\alpha$  particles. Small  $\alpha$  particles functioned as typical hard agents in a dispersion-hardened system and the volume fraction of the particles controlled the ductility. Large  $\alpha$  particles behaved like soft incoherent particles, the volume fraction having little effect on the inherent ductility of the alloy. This different behavior could be attributed to the dependence of strain-hardening behavior of  $\alpha$  particles on particle size.

The two-phase ( $\beta + \text{Ti}_3\text{Al}$ ) microstructure of the alloy with high aluminum content resulting from high-temperature aging at 900 °C exhibited a yield stress of 130 ksi and an elongation to fracture of 5%. The ductility of these microstructures was controlled by the volume fraction of the  $\text{Ti}_3\text{Al}$  particles inducing homogeneous slip. The favorable ductility properties of the microstructures with low  $\text{Ti}_3\text{Al}$  volume fraction were lost if the slip mode was changed from homogeneous slip to planar slip.

ia

UNCLASSIFIED

Security Classification

14 KEY WORDS	LINK A		LINK B		LINK C	
	ROLE	WT	ROLE	WT	ROLE	WT
Mechanical properties of Ti alloys Ductile-brittle transition Volume fraction of precipitated $\epsilon$ , $Ti_3Al$ particles Slip mode, change of Brittleness due to ordered $\beta_2$ phase						

**IMPORTANCE OF SLIP MODE FOR  
DISPERSION-HARDENED BETA TITANIUM ALLOYS**

***T. HAMAJIMA, G. LÜTJERING and S. WEISSMANN***

***RUTGERS UNIVERSITY***

***The State University of New Jersey***

Approved for public release; distribution unlimited.

ic

## FOREWORD

This report was prepared by the Materials Research Laboratory, Bureau of Engineering Research, Rutgers University, The State University of New Jersey, New Brunswick, New Jersey, under USAF Contract AF33615-69-C-1322. The contract was initiated under Project No. 7353, "Characterization of Solid Phase and Interphase Phenomena in Crystalline Substances," Task No. 735302, "Correlation of Structures and Properties." Funds for this project are supplied to the Air Force Materials Laboratory by the Office of Aerospace Research. The work was administered by the Air Force Materials Laboratory, Air Force Systems Command, Wright-Patterson Air Force Base, Ohio, with Dr. S. Fujishiro acting as Project Engineer.

This final report covers the period from October 1, 1971, to March 31, 1972. This report was submitted by the authors May 8, 1972.

This report has been reviewed and is approved.



C. T. LYNCH, Chief  
Advanced Metallurgical Studies Branch  
Metals and Ceramics Division  
Air Force Materials Laboratory

## ABSTRACT

The mechanical properties of Ti-7 Mo-7 Al and Ti-7 Mo-16 Al (in atomic per cent) were correlated to the microstructure. The mechanical properties of the alloy with low aluminum content, consisting of  $\alpha + \beta$  phases, were dependent on the size of the  $\alpha$  particles. Small  $\alpha$  particles functioned as typical hard agents in a dispersion-hardened system and the volume fraction of the particles controlled the ductility. Large  $\alpha$  particles behaved like soft incoherent particles, the volume fraction having little effect on the inherent ductility of the alloy. This different behavior could be attributed to the dependence of strain-hardening behavior of  $\alpha$  particles on particle size.

The two-phase ( $\beta + \text{Ti}_3\text{Al}$ ) microstructure of the alloy with high aluminum content resulting from high-temperature aging at 900 °C exhibited a yield stress of 130 ksi and an elongation to fracture of 5%. The ductility of these microstructures was controlled by the volume fraction of the  $\text{Ti}_3\text{Al}$  particles inducing homogeneous slip. The favorable ductility properties of the microstructures with low  $\text{Ti}_3\text{Al}$  volume fraction were lost if the slip mode was changed from homogeneous slip to planar slip.

TABLE OF CONTENTS

	<u>Page</u>
I. INTRODUCTION . . . . .	1
II. EXPERIMENTAL PROCEDURE . . . . .	1
III. RESULTS . . . . .	2
A. Mechanical Properties and Microstructure of Ti-7 Mo-7 Al . . . . .	2
B. Mechanical Properties and Microstructure of Ti-7 Mo-16 Al . . . . .	6
IV. DISCUSSION . . . . .	10
A. Change of Slip Character in Ti-7 Mo-16 Al by Second-Phase Dispersion . . . . .	10
B. Ductility Decline in Ti-7 Mo-16 Al Alloy . . . . .	11
C. Dispersion and Age-Hardening in $\alpha + \beta$ Alloys . . . . .	11
V. SUMMARY . . . . .	12
A. Ti-7 Mo-16 Al . . . . .	12
B. Ti-7 Mo-7 Al . . . . .	13
REFERENCES . . . . .	13

Preceding page blank



LIST OF ILLUSTRATIONS

<u>Figure</u>		<u>Page</u>
1	Phase Equilibria at 550 °C for the Ti-rich Corner of the Ti-Mo-Al System . . . . .	1
2	Dependence of Elongation to Fracture and Yield Stress on Aging Time at 800 °C in Ti-7 Mo-7 Al . . . . .	3
3	Dependence of Elongation to Fracture on Volume Fraction of $\alpha$ Particles in Ti-7 Mo-7 Al . . . . .	3
4	Fracture Surfaces of $\alpha + \beta$ Specimens of Ti-7 Mo-7 Al Disclosed by Scanning Electron Microscopy. 1000x. a) 0.5 h 800 °C. b) 50 h 800 °C . . . . .	4
5	Ti-7 Mo-7 Al. Transmission Electron Micrographs Showing the Dependence of Slip Mode on Volume Fraction of $\alpha$ Particles. a) 0.5 h 800 °C. Homogeneous Distribution of Dislocations. 25,000x. b) 50 h 800 °C. Inhomogeneous Slip between $\alpha$ Particles. 47,000x. . . . .	4
6	Effect of Aging on Size and Distribution of $\alpha$ Particles in Ti-7 Mo-7 Al. Light Micrographs. 1300x. a) 50 h 800 °C, b) 24 h 830 °C → 100 h 800 °C. c) 24 h 830 °C → 100 h 750 °C . . . . .	5
7	Ti-7 Mo-7 Al. Transmission Electron Micrographs Showing Dislocation Densities in $\alpha$ Particles. a) Undeformed. 40,000x. b) Deformed; $\alpha$ Particle Size $\approx 3 \mu$ . 30,000x. c) Deformed; $\alpha$ Particle Size $\approx 0.4 \mu$ . 77,000x. . . . .	6
8	Dependence of Elongation to Fracture and Yield Stress on Annealing Temperature in Ti-7 Mo-16 Al . . . . .	7
9	Fracture Modes Disclosed by Scanning Electron Microscopy in Ti-7 Mo-16 Al. 3000x. a) 2 h 1200 °C/20 °C. b) 24 h 910 °C/20 °C. c) 24 h 850 °C/20 °C . . . . .	8
10	Ti-7 Mo-16 Al. Light Micrographs Showing Change in Slip Distribution from Planar to Wavy Slip Induced by $Ti_3Al$ Particles. 250x. a) 2 h 1200 °C/20 °C. b) 24 h 910 °C/20 °C . . . . .	8
11	Ti-7 Mo-16 Al. Transmission Electron Micrographs Showing Dependence of Slip Mode on Volume Fraction of $Ti_3Al$ Particles. 30,000x. a) 24 h 850 °C. Inhomogeneous Slip between $Ti_3Al$ Particles. b) 24 h 910 °C. Homogeneous Distribution of Dislocations . . . . .	9
12	Slip Mode in Ti-7 Mo-16 Al Slowly Cooled from 980 °C → 910 °C/20 °C to Coarsen the $Ti_3Al$ Particles. a) Light Micrograph Showing Distribution of Surface Slip. 1200x. b) Transmission Electron Micrograph Showing Planar Arrangement of Dislocations. 27,000x . . . . .	10
13	Ti-7 Mo-16 Al. Electron Diffraction Patterns of a Specimen Slowly Cooled from 980 °C → 910 °C/20 °C. a) $\beta_2$ Reflections (Arrow) Present in Areas Removed from $Ti_3Al$ Particles. b) $\beta_2$ Reflections Missing in Areas Close to $Ti_3Al$ Particles . . . . .	10

## I. INTRODUCTION

The metastability which occurs upon quenching of  $\beta$ -stabilized titanium alloys constitutes the basis of a series of precipitation-hardened commercial alloys. In restricted composition ranges (Ref. 1), however, the strength properties of these alloys are greatly impeded by the occurrence of the  $\omega$  phase. This brittle phase is particularly deleterious to mechanical properties when alloys of higher solute content are tempered after quenching (Ref. 2). Williams, Hickman and Marcus (Ref. 3) have shown that volume fractions of the  $\omega$  phase higher than 0.6 result in complete embrittlement of  $\beta$ -phase titanium alloys. Even when the  $\omega$  phase is a small amount, aged  $\alpha$ - $\beta$  titanium alloys, viz., Ti-6 Al-4 V, exhibit weaknesses, particularly in the elevated temperature range, which are associated with the softness of large  $\alpha$  grains relative to the aged  $\alpha + \beta$  matrix, and which frequently lead to void formation at the grain boundaries or the  $\alpha$ - $\beta$  interfaces (Ref. 4). Recent studies of phase equilibria of the titanium-rich corner of the Ti-Mo-Al system by Hamajima, Lütjering and Weissmann (Ref. 5) have disclosed that with increasing aluminum concentration the  $\alpha$  phase can be entirely suppressed in ternary Ti-Mo-Al alloys and that the phase equilibria, as shown in Fig. 1, are greatly dependent on the presence of the  $Ti_3Al$  phase. In particular at elevated temperatures (850 °C-950 °C) the aluminum-rich alloys exhibit a phase field in which the  $\beta$  phase was shown to be in equilibrium only with the  $Ti_3Al$  phase. In view of these developments it appeared to be desirable to investigate the mechanical properties of the various microstructures in the Ti-rich corner of the ternary Ti-Mo-Al system. This paper aims to give an account of such a study.

## II. EXPERIMENTAL PROCEDURE

Sheet samples with nominal compositions (in atomic per cent) of Ti-7 Mo, Ti-7 Mo Al, and Ti-7 Mo-16 Al were obtained from the Titanium Metals Corporation of America. The initial and final rolling temperatures were 2000 °F and 1750 °F for the alloy containing 16% Al and 1850 °F and 1450 °F for the alloy with 7% Al. The details of temperatures and times for the various heat treatments were given in the results. All specimens were sealed in evacuated quartz tubes and after various heat treatments were quenched to room temperature by cracking the quartz tubes in water.

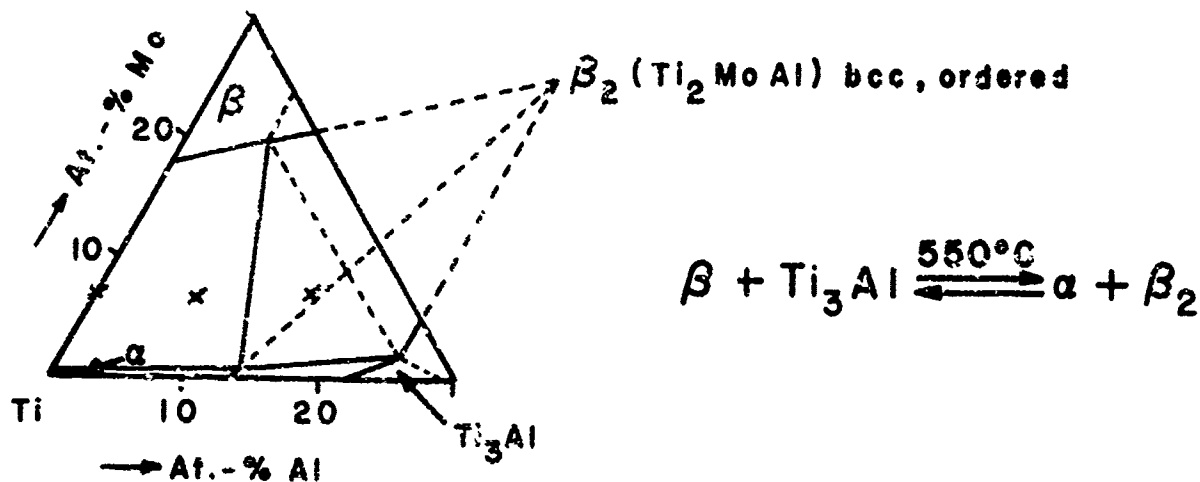


Figure 1. Phase Equilibria at 550 °C for the Ti-rich Corner of the Ti-Mo-Al System (Ref. 5).

Table 1

DEPENDENCE OF MECHANICAL PROPERTIES ON PARTICLE PARAMETERS OF  
 $\alpha$  PRECIPITATES IN Ti-7% Mo-7% Al

Heat Treatment	$\alpha$ -Particle Parameters			Mechanical Properties	
	Size ( $\mu$ )	Inter- particle Distance* ( $\mu$ )	Volume Fraction (%)	Yield Stress ( $\sigma_{0.2}$ ) (ksi)	Elongation to Fracture ( $\epsilon$ ) (%)
2 h 1000°C/20°C	--	--	--	70	7.5
0.5 h 800°C/20°C	0.4	$\approx 2.3$	10	90	4
50 h 800°C/20°C	1	$\approx 1$	35	100	1
I   24 h 830°C $\rightarrow$   100 h 800°C/20°C	3	$\approx 4$	30	86	15
II   24 h 830°C $\rightarrow$   100 h 750°C/20°C	3	$\approx 1.5$	45	100	16

\*Measured linear surface-to-surface interparticle distance.

The tensile tests were performed at room temperature on an Instron tester using a strain rate of  $4 \times 10^{-5}$  sec<sup>-1</sup>. The tensile specimens had the dimensions 0.04" x 0.25", and a gage length of 0.8". The specimens for transmission electron microscopy were prepared by electrolytic thinning, following the procedure by Blackburn and Williams (Ref. 6). The operating voltage of the electron microscope was 200 kv. The fracture surface of the specimens was investigated by scanning electron microscopy.

### III. RESULTS

#### A. Mechanical Properties and Microstructure of Ti-7 Mo-7 Al

Specimens quenched from 1000 °C to room temperature, thus having a single  $\beta$ -phase structure (Ref. 5), exhibited a yield stress ( $\sigma_{0.2}$ ) of 70 ksi and an elongation to fracture of about 7.5% (see Table 1). Aging these quenched specimens at low temperatures in the range of 350 °C-450 °C precipitated the  $\alpha$  phase from the  $\beta$  matrix (Ref. 5). As expected, this treatment rendered extreme brittleness to the alloy, the plastic elongation to fracture being zero. Aging above 450 °C produced two-phase ( $\alpha + \beta$ ) microstructures (Ref. 5). The mechanical properties, elongation to fracture  $\epsilon$  and  $\sigma_{0.2}$  yield stress, as a function of isothermal annealing at 800 °C, are shown in Fig. 2. It will be noted that, while the yield stress increased slightly with aging time, the ductility decreased to zero, as shown by the decline of the  $\epsilon$  curve. This decline of  $\epsilon$  is a characteristic feature of dispersion-hardened alloys and is encountered when the volume fraction of the dispersed phase, incoherent with the matrix, is increased and the interparticle distance decreased. Figure 3 demonstrates this dependence of the elongation to fracture on the volume fraction  $f$  of the  $\alpha$  particles precipitated in the  $\beta$  matrix at 800 °C. The volume fractions as well as

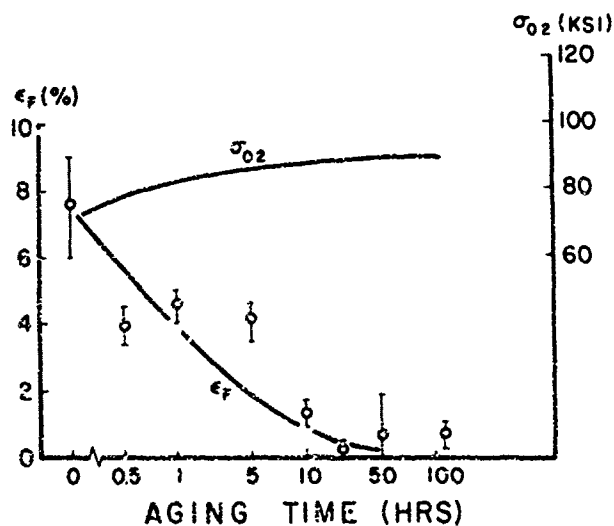


Figure 2. Dependence of Elongation to Fracture and Yield Stress on Aging Time at 800 °C in Ti-7 Mo-7 Al.

particle sizes and interparticle distances were determined by light microscopy. These particle parameters are listed in Table 1 for two characteristic examples of aging times, namely, 0.5 hours and 50 hours at 800 °C. It can be seen from Table 1 that the  $\alpha$ -particle size was quite small (0.4  $\mu$  to 1  $\mu$ ) and that the interparticle distance decreased with increasing aging time.

It is interesting to compare by scanning electron microscopy the nature of the fracture surface of the macroscopically ductile  $\alpha + \beta$  specimens which, when annealed at 800 °C for only half an hour, contained a low volume fraction of  $\alpha$  particles with the fracture surface of the macroscopically more brittle specimens, aged at the same temperature for 50 hours (volume fraction 35%; see Table 1). Comparison of Figs. 4a and 4b will show that there is no essential difference in the fracture mode between the ductile and the brittle specimens. Both exhibited the characteristic dimple type of fracture. The difference between ductility and brittleness, therefore, does not appear to lie in a difference of fracture mode but, in analogy to other dispersion-hardened systems, viz., Ni-Al<sub>2</sub>O<sub>3</sub> (Ref. 7), appears to be related to the difference in slip mode. In dispersion-hardened systems, the ductile alloys display a homogeneous distribution of slip, while brittle alloys are characterized by an inhomogeneous slip

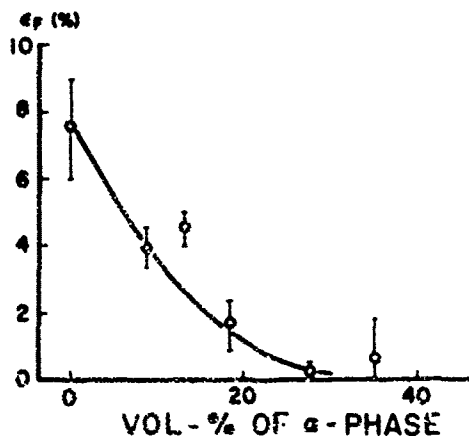
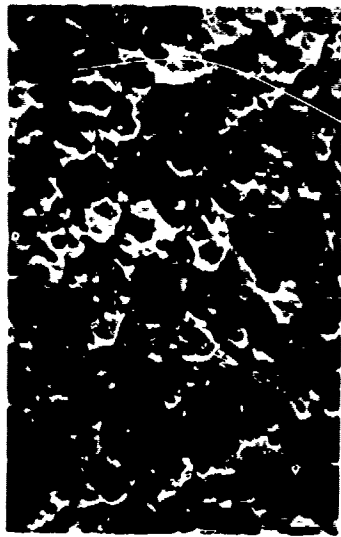
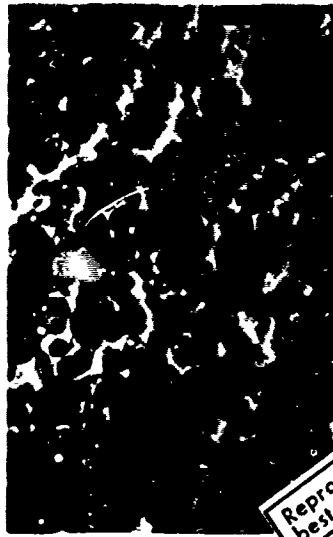


Figure 3. Dependence of Elongation to Fracture on Volume Fraction of  $\alpha$  Particles in Ti-7 Mo-7 Al.



a)



b)

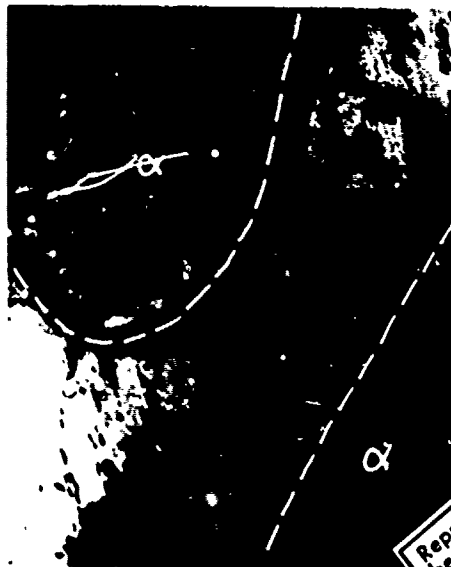
Reproduced from  
best available copy.

Figure 4. Fracture Surfaces of  $\alpha + \beta$  Specimens of Ti-7 Mo-7 Al Disclosed by Scanning Electron Microscopy. 1000x. a) 0.5 h 800 °C. b) 50 h 800 °C.

distribution. Corroborative evidence that the slip mode has been changed in the  $\alpha + \beta$  alloy by the increase of volume fraction of the precipitated  $\alpha$  particles is shown in the electron micrographs (Figs. 5a and 5b) of the fractured specimens. The specimens with a low  $f$  value exhibited a microstructure with homogeneous distribution of dislocations (Fig. 5a), while the specimens with a large  $f$  value exhibited an inhomogeneous distribution (Fig. 5b).



a)



b)

Reproduced from  
best available copy.

Figure 5. Ti-7 Mo-7 Al. Transmission Electron Micrographs Showing the Dependence of Slip Mode on Volume Fraction of  $\alpha$  Particles. a) 0.5 h 800 °C. Homogeneous Distribution of Dislocations. 25,000x. b) 50 h 800 °C. Inhomogeneous Slip between  $\alpha$  Particles. 47,000x.

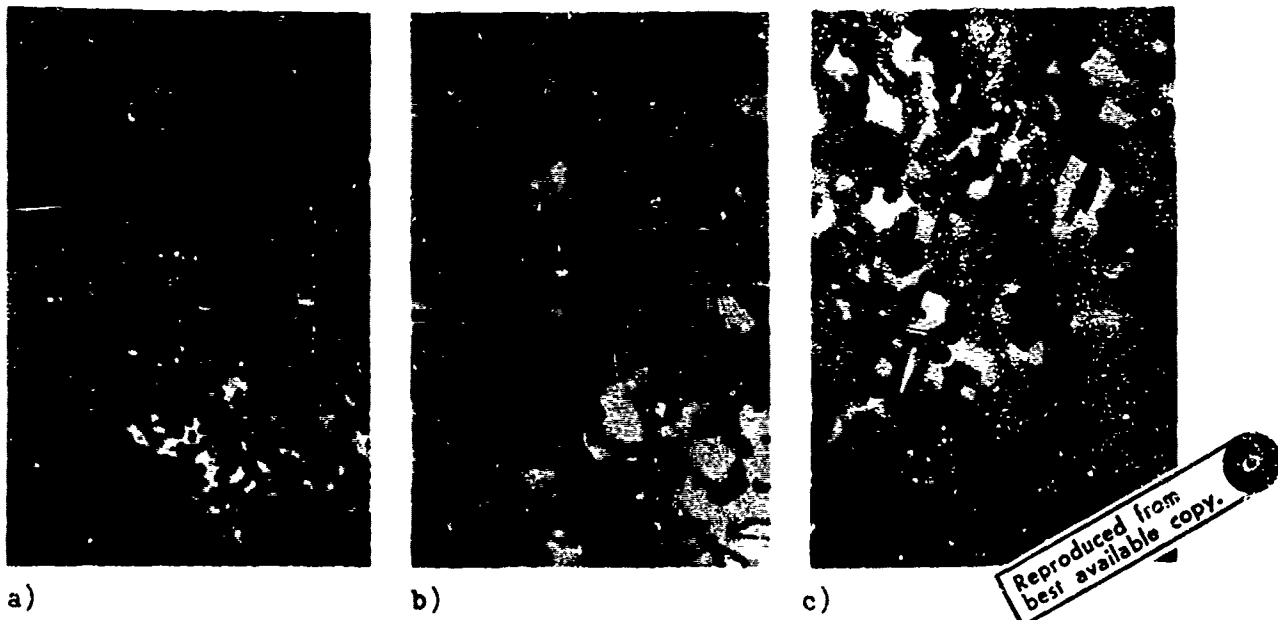


Figure 6. Effect of Aging on Size and Distribution of  $\alpha$  Particles in Ti-7 Mo-7 Al. Light Micrographs. 1300x. a) 50 h 800 °C. b) 24 h 830 °C → 100 h 800 °C. c) 24 h 830 °C → 100 h 750 °C.

It was found that with long aging times at 800 °C the ductility tended to increase again, while the volume fraction remained constant. It was observed that this ductility increase was associated with coarsening of the  $\alpha$  precipitates. To test this observation a different aging treatment was used in order to enhance the coarsening process at constant volume fraction. The specimens were aged at the higher temperature of 830 °C for 24 hours to decrease the number of nucleation sites of  $\alpha$  particles and subsequently the aging temperature was lowered to the previous temperature of 800 °C. The specimens were held at 800 °C for 100 hours to insure precipitation of the constant volume fraction. It will be seen from Table 1 that by means of this aging treatment, denoted as aging treatment I, both the average size and interparticle distance of  $\alpha$  particles were increased from 1 to about 4  $\mu$  as compared to the specimens aged directly at 800 °C for 50 hours, while the volume fraction remained approximately constant. The results of the tensile tests are also shown in Table 1. These results show that the elongation to fracture increased to the high value of 15%.

The observed increase in ductility at once raised the question whether it was caused by the increase of interparticle distance or by the increase in particle size, both resulting from the coarsening process. To decide between these two possibilities a different sequence of aging treatment was applied. The specimens were again aged at 830 °C for 24 hours but subsequently cooled to the lower aging temperature of 750 °C and held for 100 hours (aging treatment II). The latter step was introduced to increase the volume fraction and, therefore, to decrease the interparticle distance between the  $\alpha$  precipitates while maintaining a large particle size. The representative micrographs of Figs. 6a, 6b and 6c may serve to visualize the relationship of particle size, interparticle distance and volume fraction resulting from the various aging treatments list in Table 1. Examination of Table 1 shows that while the volume fraction increased from 30% to 45% and the interparticle distance decreased as a result of aging treatment II,

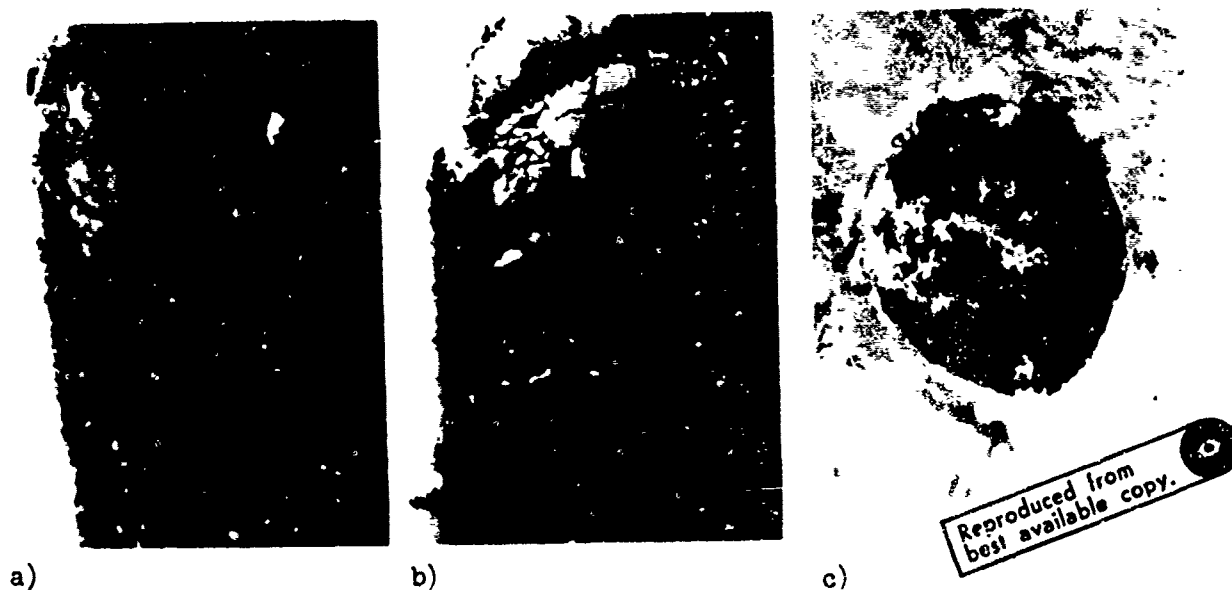


Figure 7. Ti-7 Mo-7 Al. Transmission Electron Micrographs Showing Dislocation Densities in  $\alpha$  Particles. a) Undeformed. 40,000x. b) Deformed;  $\alpha$  Particle Size  $\approx 3 \mu$ . 30,000x. c) Deformed;  $\alpha$  Particle Size  $\approx 0.4 \mu$ . 77,000x.

the elongation to fracture remained virtually invariant. It is quite evident, therefore, that the observed increase of ductility in the  $\alpha + \beta$  alloy was due to the size increase of the  $\alpha$  particles and not the increase of interparticle distance.

It appears that upon deformation the  $\alpha$  particles functioned as hard particles if their size was  $1 \mu$  or smaller and that they behaved like soft particles if their size was  $3 \mu$ . To elucidate the point why the  $\alpha$  particles, depending on their size, acted as hard or soft particles in the moment the yield stress of the  $\beta$  matrix was reached, the dislocation density within the  $\alpha$  particles was investigated by transmission electron microscopy. The undeformed  $\alpha$  particles showed, independent of their size, only a few dislocations, as shown in Fig. 8a. A drastic difference in dislocation density between small and large  $\alpha$  particles was found in slightly deformed specimens (Figs. 7b and 7c). Whereas the dislocation density within the  $\alpha$  particles remained relatively low for a specimen having an average  $\alpha$  particle size of  $3 \mu$  (Fig. 7b), a tremendously high density of dislocations was found within the  $\alpha$  particles in specimens having a small particle size of about  $0.4 \mu$  (Fig. 7c).

#### B. Mechanical Properties and Microstructure of Ti-7 Mo-16 Al

It has been shown that quenching of this alloy from the  $\beta$ -phase field produced fine  $\beta_2$  particles. These are coherent with the  $\beta$  matrix and have a CsCl type of structure (Ref. 5). It has already been demonstrated by Böhm and Löhberg (Ref. 8) many years ago that the presence of this phase resulted in extreme brittleness of Ti-Mo-Al alloys. This brittle behavior was also confirmed in this study, as can be seen from Fig. 8, where the mechanical properties are plotted as a function of annealing temperatures. Specimens annealed at temperatures above  $950^\circ \text{C}$  ( $\beta$ -phase field) exhibited zero plastic elongation.

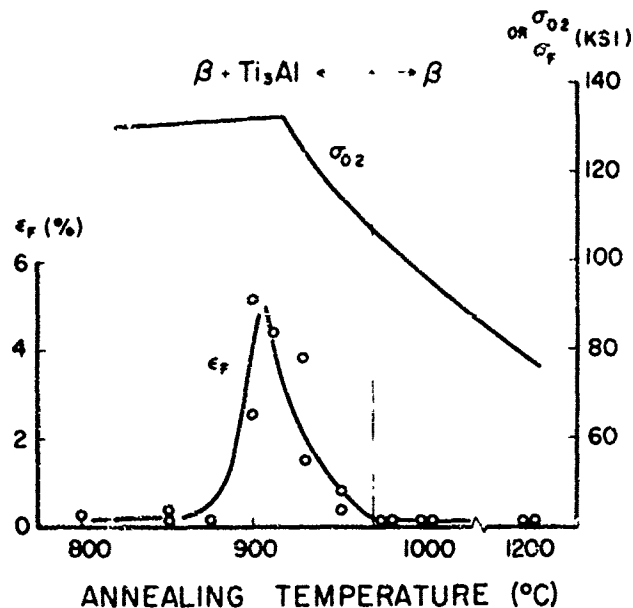


Figure 8. Dependence of Elongation to Fracture and Yield Stress on Annealing Temperature in Ti-7 Mo-16 Al.

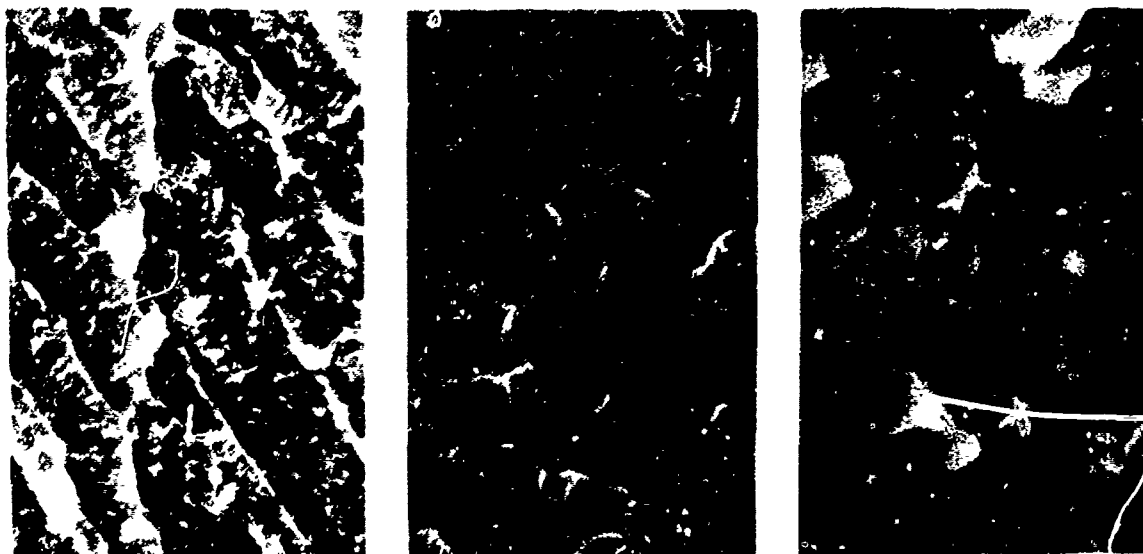
Since specimens aged below 550 °C contained, besides  $\alpha$  particles within the  $\beta$  matrix, also the  $\beta_2$  phase (Fig. 1), they all displayed extreme brittleness. Although aging above 550 °C resulted in the elimination of the  $\beta_2$  phase and the establishment of a three-phase equilibrium of  $f + \alpha + Ti_3Al$  (Ref. 5), the alloys up to the aging temperature of about 800 °C were still brittle and in this range of aging temperature the brittleness derived principally from the large volume fraction of  $\alpha$  and  $Ti_3Al$  particles.

A remarkable change in mechanical properties took place, however, when the Ti-7 Mo-16 Al alloy was aged between 850 °C and 950 °C, as may be seen from Fig. 8. It has been shown in the study of phase equilibria (Ref. 5) that this range of aging temperature corresponds to the phase field in which only  $f$  and  $Ti_3Al$  are in equilibrium. In this temperature range the per cent elongation increased from zero (total brittleness) to about 5% at 910 °C, with a concomitant increase of  $\sigma_{0.2}$  to about 130 ksi. Increasing the aging temperature after attainment of these maxima resulted in a decline of both flow stress and per cent elongation, the latter again reaching zero values above 950 °C.

Since the maxima in mechanical properties attained at the high aging temperature of 900 °C may be of considerable interest from a technological viewpoint, it appeared to be desirable to test the structural stability with respect to subsequent low-temperature aging. Consequently the specimens which were aged at 910 °C for 24 hours were subsequently aged at 400 °C for 100 hours and tested. The elongation to fracture remained invariant ( $\epsilon = 5\%$ ) and the yield strength was increased to  $\sigma_{0.2} = 160$  ksi. The reason for this additional strength increase is attributed to the decomposition of the  $\beta$  phase, while the large  $Ti_3Al$  particles remained unchanged.

If one compares the fracture mode of as-quenched specimens containing  $\beta$  and  $\beta_2$  phases (Fig. 9a) with specimens aged in the temperature range of 850 °C to 950 °C, containing  $\beta + Ti_3Al$  (Figs. 9b and 9c), one becomes immediately convinced that the fracture mode has changed from a shear type to a dimple type. This change in fracture mode is consistent with the observed ductility rise





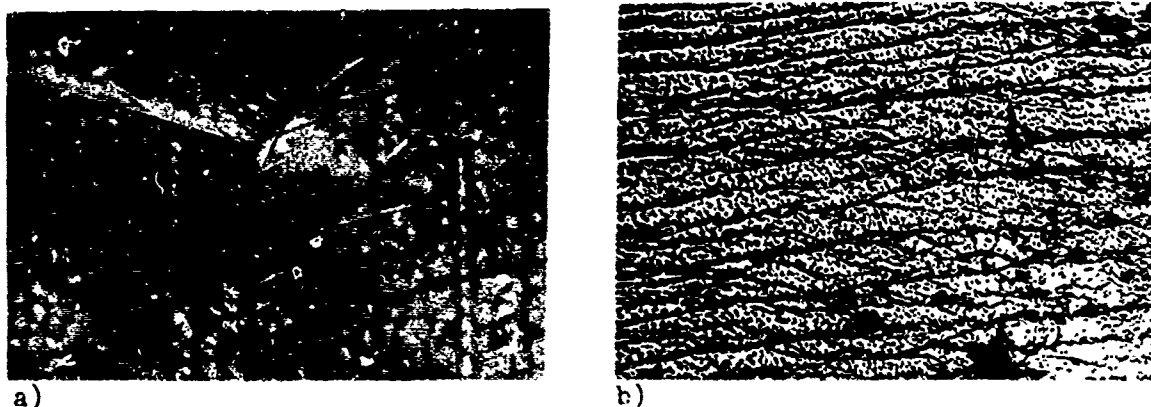
a) b) c)

Figure 9. Fracture Modes Disclosed by Scanning Electron Microscopy in Ti-7 Mo-16 Al. 3000x. a) 2 h 1200 °C/20 °C. b) 24 h 910 °C/20 °C. c) 24 h 850 °C/20 °C.

Reproduced from best available copy.

shown in Fig. 8. The change in fracture mode was also manifested by a characteristic change in the distribution of slip lines when metallographic surface studies of the fractured specimens were carried out. As shown in Fig. 10a, the as-quenched specimen exhibited a few high slip steps which were widely separated from each other. This type of distribution of slip traces is characteristic of brittle alloys hardened by coherent precipitates (Ref. 9). By contrast, the slip traces of the specimen aged at about 900 °C displayed a wavy slip configuration consonant with the observed ductility rise (Fig. 10b).

Detailed studies of the microstructures were performed corresponding to the range of aging temperatures (850 °C to 950 °C) over which the rise and decline of ductility was observed. Figure 11a shows the electron micrograph of a speci-



a) b)

Figure 10. Ti-7 Mo-16 Al. Light Micrographs Showing Change in Slip Distribution from Planar to Wavy Slip Induced by  $Ti_3Al$  Particles. 250x. a) 2 h 1200 °C/20 °C. b) 24 h 910 °C/20 °C.

Reproduced from best available copy.

Reproduced from  
best available copy.



a)



b)

Figure 11. Ti-7 Mo-16 Al. Transmission Electron Micrographs Showing Dependence of Slip Mode on Volume Fraction of  $Ti_3Al$  Particles. 30,000x. a) 24 h 850 °C. Inhomogeneous Slip between  $Ti_3Al$  Particles. b) 24 h 910 °C. Homogeneous Distribution of Dislocations.

men aged at 850 °C for 24 hours and then fractured. This aging temperature corresponds to the region where zero ductility was observed (see Fig. 8). At this temperature the volume fraction of  $Ti_3Al$  particles was high (approximately 50%) and the interparticle spacing was small, having an average value of about 0.5  $\mu$ . It was observed that in these aged specimens the slip activity was principally confined to interparticle regions and, as may be seen from Fig. 11a, the dislocations interconnected the  $Ti_3Al$  particles by virtually straight lines.

The electron micrograph of Fig. 11b shows the dislocation configuration of a deformed specimen aged at 910 °C for 24 hours, a temperature which corresponded to the maximum in ductility (Fig. 8). At this aging temperature the volume fraction of  $Ti_3Al$  particles had undergone a considerable decline to about 15% and was accompanied by a corresponding increase in interparticle spacing to about 5  $\mu$ . Concomitant with this increase in interparticle distance the distribution of dislocations became uniform throughout the matrix. In comparing specimens aged at 850 °C and 900 °C with each other, it should be borne in mind, however, that, although the slip distribution changed from inhomogeneous to homogeneous and at the same time the ductility changed from 0% to 5%, the fracture mode remained the same, as can be seen by comparing Figs. 9b and 9c.

The slip distribution obtained from fractured specimens corresponding to the higher annealing temperature which induced the decline in ductility is shown in Fig. 12. Both the surface slip disclosed by light microscopy and the distribution of dislocations revealed by electron microscopy gave evidence of a planar slip mode. To elucidate the contributing factors for this planar arrangement of dislocations a series of selected area diffraction studies was carried out as a function of distance from the precipitated  $Ti_3Al$  particles. It was observed that diffraction patterns taken from areas removed from the  $Ti_3Al$  particles disclosed superlattice reflections pertaining to the  $\beta_2$  structure, such as that pointed out by the arrow of Fig. 13a. On the other hand, diffraction patterns taken in close vicinity to  $Ti_3Al$  particles, such as that shown in Fig. 13b, displayed only  $\beta$  reflections and none of the reflections pertaining to the ordered  $\beta_2$  structure was observed.

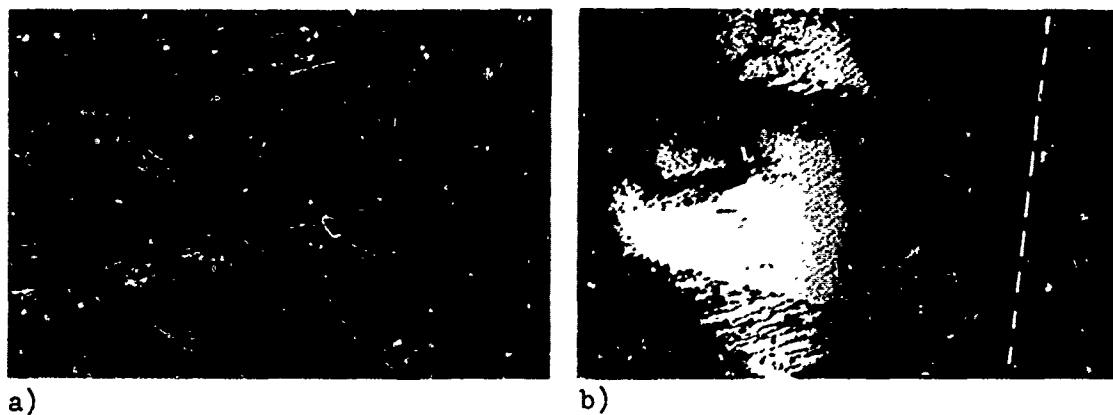


Figure 12. Slip Mode in Ti-7 Mo-16 Al Slowly Cooled from 980 °C → 910 °C/20 °C to Coarsen the Ti<sub>3</sub>Al Particles. a) Light Micrograph Showing Distribution of Surface Slip. 1200x. b) Transmission Electron Micrograph Showing Planar Arrangement of Dislocations. 27,000x.

Reproduced from  
best available copy.

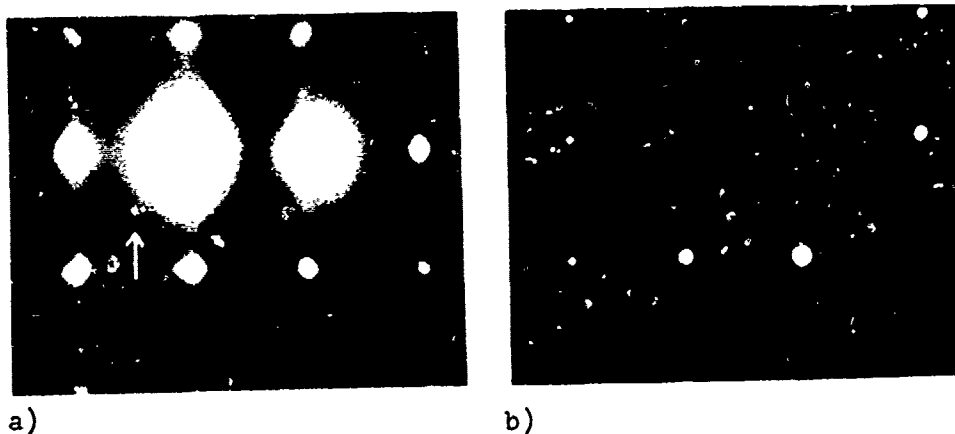


Figure 13. Ti-7 Mo-16 Al. Electron Diffraction Patterns of a Specimen Slowly Cooled from 980 °C → 910 °C/20 °C. a)  $\beta_2$  Reflections (Arrow) Present in Areas Removed from Ti<sub>3</sub>Al Particles. b)  $\beta_2$  Reflections Missing in Areas Close to Ti<sub>3</sub>Al Particles.

#### IV. DISCUSSION

##### A. Change of Slip Character in Ti-7 Mo-16 Al by Second-Phase Dispersion

Perhaps the most interesting result which emerged from this study is the rise in ductility from total brittleness to about 5%, accompanied by a slight increase in yield strength when the aluminum-rich alloy was aged from about 850 °C to 910 °C. It could be shown that this increase in strength properties derived from the particles of the intermetallic Ti<sub>3</sub>Al phase dispersed in the  $\beta$  matrix and that in this temperature range only Ti<sub>3</sub>Al coexisted with the  $\beta$

phase. When the strength properties were optimized (910 °C; see Fig. 8) the slip mode was changed from an inhomogeneous to a homogeneous distribution. At the lower aging temperature of 850 °C, however, such homogeneous slip distribution could not be obtained because of the large volume fraction of the Ti<sub>3</sub>Al particles of about 50%. For that volume fraction of Ti<sub>3</sub>Al particles the interparticle distance became so short that on deformation of the alloy the dislocations which were generated from the particle-matrix interfaces and influenced by the nearby particles interconnected with adjacent Ti<sub>3</sub>Al particles directly (Fig. 11a). Consequently this slip mode gave rise to an inhomogeneous distribution of local plastic deformation and this inhomogeneous slip distribution was reflected by the low ductility value of the alloy (Fig. 8).

The optimum strength values could be obtained only when the interparticle distance was appropriately increased by increasing the aging temperature to 910 °C and thus decreasing the volume fraction of precipitated Ti<sub>3</sub>Al. Such distribution of Ti<sub>3</sub>Al particles in the β matrix insured homogeneous slip, because upon deformation of the alloy the dislocations generated from the particle-matrix interfaces nucleated and moved in a statistical manner (Fig. 11b).

It was also shown that specimens aged for the maxima in strength properties did not lose these favorable properties when aged at the lower temperature of 400 °C. Indeed, the yield stress increased to 160 ksi due to the decomposition of the β matrix. The elongation to fracture, however, remained invariant (ε = 5%), giving corroborative evidence that the ductility properties were governed by the large Ti<sub>3</sub>Al particles homogeneously distributed throughout the matrix.

#### B. Ductility Decline in Ti-7 Mo-16 Al Alloy

The decline of ductility between 900 °C and 950 °C (Fig. 8) was not associated with a drastic decline in volume fraction of Ti<sub>3</sub>Al precipitates but rather with the coarsening of the particles and with the concomitant increase in interparticle distance and the appearance of the non-equilibrium β<sub>2</sub> precipitates which nucleated upon quenching. The latter in turn gave rise to a change in slip mode, altering it from a wavy, homogeneous distribution (Fig. 10b) to a planar, inhomogeneous distribution (Fig. 12a). The selected area diffraction pattern taken in the vicinity of the large Ti<sub>3</sub>Al particles (Fig. 13b) showed that in these areas there existed a true phase equilibrium between the Ti<sub>3</sub>Al phase and the β matrix. Owing to the aluminum depletion by the Ti<sub>3</sub>Al particles the non-equilibrium β<sub>2</sub> phase, which corresponds to the composition of Ti<sub>2</sub>MoAl (Ref. 8), could not be formed upon quenching. In areas removed from the Ti<sub>3</sub>Al particles the selected area diffraction pattern of Fig. 13a showed the existence of the non-equilibrium β<sub>2</sub> phase. The planar slip characteristics observed in this temperature range (Fig. 12b) are attributed to the presence of β<sub>2</sub>.

No attempt has been made as yet to vary systematically the aluminum content so as to achieve optimization of volume fraction, interparticle distance and mechanical properties and to eliminate non-equilibrium conditions.

#### C. Dispersion and Age-Hardening in α + β Alloys

It is interesting to note that a dispersion-hardening effect was also obtained in the α + β specimens of the aluminum-poor ternary alloy (Ti-7 Mo-7 Al) by isothermal aging at 800 °C (Fig. 2). This dispersion-hardening effect on the β matrix was induced by a high strain-hardening of the small α particles upon deformation (Fig. 7c). This phenomenon appears to be of particular interest,

since  $\alpha$  particles are usually associated with softness relative to the  $\beta$  matrix. In the present case the strength of the  $\beta$ -matrix can be approximated by taking the value of the as-quenched specimens ( $\sigma_{0.2} = 70$  ksi; see Table 1) or the  $\sigma_{0.2}$  value of the binary Ti-7% Mo alloy (60 ksi). By comparison the  $\sigma_{0.2}$  value of the  $\alpha$  phase depleted of molybdenum can be assumed to be close to the value for the binary Ti-9.7% Al alloy ( $\sigma_{0.1} = 40$  ksi) (Ref. 9). It appears to be possible, therefore, to obtain a dispersion-hardening effect in  $\alpha + \beta$  alloys if the  $\alpha$  precipitates are kept sufficiently small. It is noteworthy that in this dispersion-hardened system the loss of ductility (Fig. 3) was again associated with a change in slip mode (Figs. 5a and 5b) conditioned by the increase of volume fraction of  $\alpha$  particles and concomitant decrease of interparticle distance.

When, however, the precipitated  $\alpha$  particles were coarsened by prolonged aging, the volume of the single  $\alpha$  particles was increased by a factor of ten, they did not undergo drastic strain-hardening upon deformation and the ductility of the  $\alpha + \beta$  alloy was increased from about 1% to 15% (Table 1). Thus when the  $\alpha$  particles were small they behaved like typical hard agents in a dispersion-hardening system, and as such the ductility of the  $\alpha + \beta$  alloy was determined by the volume fraction of the  $\alpha$  particles. Upon coarsening, however, the role which the  $\alpha$  particles played in the strengthening mechanism underwent a change, for they assumed now a function typical of soft, incoherent precipitates.

This different behavior should also be reflected in the macroscopic strain-hardening behavior of the specimens. Thus the difference  $\sigma_{1.0} - \sigma_{0.2}$  was for specimens having an average  $\alpha$ -particle size of  $0.4 \mu$  (0.5 h 800 °C/20 °C), 15 ksi as compared to specimens with an  $\alpha$ -particle size of  $3 \mu$  (24 h 830 °C → 100 h 750 °C/20 °C), where the same stress difference was only 2 ksi.

The increase in yield stress of the various ( $\alpha + \beta$ ) specimens over the single phase  $\beta$  structure (Table 1) seems to be determined by the interparticle distance. That no difference in ductility was found between the two different volume fractions of large  $\alpha$  particles (compare specimens I and II in Table 1) is certainly true only as long as the  $\beta$  phase is the matrix. It would be interesting to increase the volume fraction of the  $\alpha$  phase to an extent where the  $\alpha$  phase would take the position of the matrix.

## V. SUMMARY

A study relating mechanical properties of Ti-7 Mo-16 Al and Ti-7 Mo-7 Al (in at %) alloys to microstructures was carried out and the results obtained were as follows.

### A. Ti-7 Mo-16 Al

1) The ductility rose from total brittleness to about 5% elongation when the alloy was aged in the high-temperature, two-phase region consisting of  $\beta + \text{Ti}_3\text{Al}$  precipitates. This ductility increase was accompanied by a rise in yield strength to about 130 ksi.

2) The optimum values of the strength properties were obtained at the aging temperature of 910 °C when the  $\text{Ti}_3\text{Al}$  particles dispersed in the  $\beta$  matrix had the proper interparticle distance to insure a homogeneous slip distribution. These optimum values in strength properties were not lost upon subsequent low-temperature aging at 400 °C for 100 hours.

3) The decline of the ductility at the lower and higher aging temperatures of 850° and 950° C was due to the large volume fraction of Ti<sub>3</sub>Al particles and the presence of the coherent, non-equilibrium  $\beta_2$  particles between the Ti<sub>3</sub>Al particles, respectively. In both cases the decline of ductility was associated with a change in the slip mode from a homogeneous to an inhomogeneous distribution.

4) Quenching from the single  $\beta$ -phase field resulted in extreme brittleness due to the presence of coherent, ordered  $\beta_2$  particles. The presence of these particles was the reason for a planar slip mode.

#### B. Ti-7 Mo-7 Al

1) After solution treatment and quenching, isothermal aging in the two-phase field ( $\alpha + \beta$ ) at 800° C resulted in a drastic decline of ductility from about 7.5% to 1%, if the  $\alpha$  particles were kept sufficiently small (1  $\mu$ ). This decline was dependent on the amount of volume fraction of precipitated  $\alpha$  particles. This behavior is typical for dispersion-hardened materials.

2) Upon coarsening of the  $\alpha$  particles at 800° C the ductility increased to 15%. This increase was controlled by the larger size of  $\alpha$  particles (3  $\mu$ ) and not by the larger interparticle distance. In this case the  $\alpha$  particles acted as soft, incoherent particles.

3) A size-dependent strain-hardening behavior of the  $\alpha$  particles can explain why the  $\alpha$  particles, depending on their size, acted as hard or soft particles upon reaching the yield stress of the  $\beta$  matrix.

#### REFERENCES

1. C. A. Luke, R. Taggart and D. H. Polonius, *Trans. ASM* 50, 455 (1958).
2. Yu, A. Bagaryatskii and G. I. Nosova, *Fiz. Metall. Metalloved* 13, 415 (1962).
3. J. C. Williams, B. S. Hickman and H. L. Marcus, *Met. Trans.* 2, 1913 (1971).
4. H. Margolin, P. A. Farrar and M. A. Greenfield, *The Science, Technology and Application of Titanium*, R. I. Jaffee and N. E. Promisel, eds., Pergamon Press, 1970, pp. 795-808.
5. T. Hamajima, G. Lütjering and S. Weissmann, *Microstructure and Phase Relations for Ti-Mo-Al Alloys*, Technical Report, AFML-TR-71-236, November, 1971.
6. M. J. Blackburn and J. C. Williams, *Trans. TMS-AIME* 239, 287 (1967).
7. G. Lütjering, private communication.
8. H. Böhm and K. Löhberg, *Z. Metallkde.* 49, 173 (1958).
9. G. Lütjering and S. Weissmann, *Acta Met.* 18, 785 (1970).